CROATICA CHEMICA ACTA CCACAA 61 (2) 331—346 (1988)

YU ISSN 0011-1643
CCA-1797 UDC 543.42
Author's Review

Characterization of Low Dimensional Materials by Raman Spectroscopy

S. Nakashima and M. Hangyo

Faculty of Engineering, Department of Applied Physics, Osaka University, Suita, Osaka 565, Japan

Received November 19, 1987

This article reviews recent advances in the Raman scattering study of one- and two-dimensional materials. The characteristic vibrational properties of the low dimensional crystals are described and various methods of characterizing these crystals are summarized. Recent experimental results on polymer crystals, inorganic chain-like crystals, layered crystals and intercalated layer crystals are presented.

I. INTRODUCTION

A class of solids known as low dimensional (one- and two-dimensional) materials has received considerable attention in recent years. The one-dimensional materials have a linear chain structure, such that the interchain force is much smaller than the intrachain forces. Their physical properties largely depend on the chain length, which is characterized by Raman scattering. A number of low dimensional crystals undergo a charge density wave (CDW) phase transition. The measurement of phonons in these materials is a powerful tool for understanding the mechanism of the CDW transition.

A prototype of two-dimensional materials is a layered crystal whose interlayer forces are much smaller than the intralayer forces. The ratio of inter- and intra-layer forces is usually of the order of $10^{-2} \sim 10^{-4}$ for layered crystals. The existence of such anisotropic forces with different strengths leads to anisotropy in mechanical, dielectric, optical and particularly electronic properties for the low dimensional materials.

Textbooks usually state that the interlayer interaction originates from van der Waals interaction. However, there are a number of materials intermediate between two- and three-dimensional materials such as GeSe, SnSe, *etc.* In these intermediate materials, covalent and/or ionic bondings, in addition to van der Waals interaction, may contribute partly to the interlayer interaction. The Raman spectroscopy is widely used to characterize the low dimensional materials, because it enables us to measure the phonon frequencies with high accuracy and then the degree of the anisotropy in the low dimensional materials is estimated.[1,2]

Because of weak interlayer forces, the intercalation of organic and inorganic molecules between layers is possible for some layered crystals. It has been found that for these materials physical properties, such as electrical,

magnetic and optical, are modified significantly by the intercalation. For chalcogenides of group IV and V elements the phase transition temperature is drastically changed by the intercalation of organic molecules.[3]

The Raman scattering is expected to provide information about the bonding nature of hosts and guests and the charge transfer between them in the intercalated layered crystals. To understand the mechanism of the intercalation and charge transfer between the host and guest, the phonon structure of intercalated materials has been studied. Recently, we have succecded in observing the internal modes of pyridine intercalated in $MnPS_3$.[4] The Raman spectra of the guest molecule have shown that there are two kinds of molecules in the van der Waals gap; physisorbed and chemisorbed molecules.

Recently, the relative intensity of the Raman bands has been used to determine the layer stacking in the CdI_2 polytyeps.[5] This determination is analogous to the X-ray diffraction analysis in which the stacking sequence is determined from a comparison of the intensities of the observed reflections with that calculated for postulated structural models. The Raman scattering analysis of polytypes can be extended to the identification of disordered layered crystals.

Raman scattering data accumulated so far and developments in the analysis have enabled us to characterize low dimensional materials quantitatively by Raman measurements. We obtain information about the dimensionality: (1) anisotropy of the binding forces, (2) strength and nature of the interlayer and interchain forces, (3) structure of the layer stacking in layered crystals, and (4) bonding nature of the intercalants and charge transfer in intercalated materials.

II. ONE-DIMENSIONAL MATERIALS

(i) Resonance Raman Spectra and Chain-Length Distribution in Polymers

It is easily conjectured that defects or impurities considerably affect the electronic properties of low dimensional materials such as polymers. If there are defects on the backbone of polymers, the overlapping of π orbitals may be interrupted. Accordingly, considerable defects on the backbone confine the π electrons within the short chains. Most of the polymers synthesized in forms of fibrils contain considerable amounts of kinks or defects.

Polyacetylene (PA), which is a typical conductive polymer, is usually obtained as fibrils with diameters of ~ 20 nm. There are two types of PA, i. e. cis-and more stable trans-PA. For trans-PA, remarkable excitation-energy dependence of Raman spectra has been observed[6-9]. When the Raman spectra are excited at 1.83 eV, two strong bands appear at ~ 1060 and ~ 1450 cm^{-1}, which are assigned to the stretching vibrations of the C—C (ν_{C-C}) and C=C ($\nu_{C=C}$) bonds, respectively.[8] These bands have tails on the high energy side. With increasing excitation energy, these tails grow and become separate peaks. In general, the Raman shift is a characteristic inherent in materials and does not depend on the excitation energy. The peculiar excitation-energy dependence observed for trans-PA is explained as follows: There are PA chains with various effective lengths in the sample, which have different

band gaps and vibrational frequencies. In the resonance Raman spectra, the scattering efficiency of the chains, which have band gaps close to the energy of the incident light, is selectively enhanced. Brivio and Mulazzi[9] calculated the dependence of the Raman spectra on the excitation energy assuming the distribution of the chain length to be expressed by two Gaussians peaked at 100 and 15 C=C bonds. The calculated spectra agreed quite well with the experimental ones.

Polydiacetylenes (PDA) are a group of polymers with backbone chains having alternative C—C, C=C and C≡C bonds. Since they are obtained by the solid state polymerization from monomer crystals, the chystal quality is excellent. Their quality is degraded by hammering or rolling a single crystal. The degraded PDA shows the upshift of the Raman lines corresponding to the C=C and C≡C stretching mode as the excitation energy increases.[10] This result is also explained by the change in the chain-length distribution. Some PDA can be solved in solvent. The PDA chains take rod- or coil-like conformations depending on the solvent and temperature, and the distribution of the effective chain length changes with the conformation. This distribution was estimated by the resonant Raman measurements.[11]

(ii) Dimensionality and Interchain Interaction

There are many crystals consisting of chain-like units. However, some of these crystals cannot be regarded as ideal one-dimensional systems. It is possible to estimate the dimensionality from the vibrational spectra, although there have been few studies aimed at evaluating the interchain interaction.

Transition metal trichalcogenides (MX_3) crystallize in chain structures, for which distorted trigonal MX_6 prisms are stacked in the chain direction. The chains are linked in a layer type structure. From the observed Raman and infrared spectra, it has been shown that the force constant between the M and X atoms in neighbouring chains within the same layer is comparable with that between the M and X atoms within the chain.[12,13] On the other hand, the force constant between the nearest neighbour atoms in the adjacent layers are weak compared with the intrachain force constant by one or two orders of magnitude.[8] Accordingly, MX_3 is considered to have an intermediate structure between the layer and chain-like crystal. This speculation is consistent with the fact that the distance between the M and X atoms in neighbouring chains is relatively short.

$(SN)_x$ is an inorganic polymer which is obtained as a single crystal. The primitive unit cell contains two chains and the inversion centre is located between the chains. Therefore, the phonon modes split into Davydov pairs owing to the interchain interaction. The splitting energy amount to 30 ~ 40 cm^{-1},[14] which indicates that $(SN)_x$ cannot be regarded as an ideal one-dimensional system.

(iii) CDW Phase Transition

Considerable attention has been paid to the CDW phase transition in low dimensional materials. Raman spectra are expected as a method for estimating the symmetry and the temperature dependence of the lattice distortion due to the CDW.

The CDW phase transition has been investigated by Raman spectroscopy for TaS_3,[15,16] $(TaSe_4)_2I$,[17-20] $(NbSe_4)_2I$,[20] $K_2Pt(CN)_4Br_{0.3} \cdot 3.2H_2O$ (KCP)[21] and $K_{0.3}MoO_3$.[22] The amplitude mode has been observed in the CDW-distorted phase for KCP,[21] $K_{0.3}MoO_3$,[22] $(TaSe_4)_2I$[17,19,20] and $(NbSe_4)_2I$.[20] The broadening of this mode when approaching the phase transition temperature was explained by the interaction between the amplitude and phase modes.[23] Tsang et al.[15] obtained the CDW gap as a function of temperature in TaS_3 from the temperature dependence of the phonon frequency and band width. However, high resolution spectra measured by Sugai[16] cast doubt on the interpretation of the temperature dependence of the spectra by Tsang *et al.* So far, the effect of the CDW phase transition on the phonon structure in one-dimensional crystals has not been well understood.

III. TWO-DIMENSIONAL MATERIALS: LAYERED CRYSTALS

(i) Evaluation of Interlayer Forces

The interlayer forces are a few orders of magnitude smaller than the intralayer forces in layered crystals. As easily understood from the lattice dynamical calculation using a linear chain model with two different force constants in a unit cell, the restoring force for the acoustic phonons propagating perpendicular to the layer is dominated by the weak interlayer force and a whole layer moves as a rigid body for this mode. Accordingly, the dispersion relations and frequencies of the acoustic phonons provide information on the strength and nature of the interlayer forces. For the layered crystals which have only a layer in the unit cell, the dispersion of acoustic phonons is estimated by the Brillouin scattering measurements. On the other hand, for layered crystals having more than one layer in the unit cell, one observes so called »rigid layer modes« which correspond to *folded modes* of zone edge phonon and/or midzone phonon modes in the basic crystal with a layer per unit cell.[1,2]

(ii) Pressure Raman Effect in Layered Crystals

The coexistence of strong and very weak forces in low dimensional materials gives rise to a peculiar pressure dependence of phonon modes. Since the strength of very weak bonding forces varies drastically with pressure, the rate of the frequency variation with pressure is larger for rigid layer modes (interlayer modes) than for the intralayer modes. In reality, weak intralayer forces often exist in layer crystals and the restoring force of the phonon modes consists of a mixture of inter- and intra-layer forces. In this case, the mode-Grüneisen parameter is expected to vary with the inverse of the squared phonon frequency:[24]

$$\gamma_i = \frac{1}{K}\frac{1}{\omega_i}\frac{d\omega_i}{dP} \propto \omega_i^{-2} \tag{1}$$

where K is the compressibility and P is the pressure. The experimental mode-Grüneisen parameter of the rigid layer modes exceeds 10 for several layered crystals. It has been experimentally shown that the variation of the mode-Grüneisen parameter in As_2S_3 and As_2Se_3 follows Eq. (1). On the other

hand, the mode Grüneisen parameters of three-dimensional materials are usually less than 5 and do not show noticeable frequency dependence.

Variation of the interlayer distance and rigid layer mode frequency under hydrostatic pressure has been measured in 4H—CdI_2 and 18R—SnS_2.[25] If we assume that the interlayer forces arise from van der Waals interaction between iodine-iodine ions in the adjacent layers, the interlayer interaction is expressed by 6-exp type potential:

$$V(r) = -\frac{C}{r^6} + B\,e^{-r/\varrho} \tag{2}$$

where r is the distance between the iodine atoms. Van der Waals constant C is given by

$$C = \frac{3}{4}\,\frac{e\hbar}{m^{1/2}}\,\frac{\alpha^2}{(\alpha/N)^{1/2}} \tag{3}$$

where α is the polarizability and N is the effective number of electrons in iodine. The restoring force of transverse rigid layer mode is given by

$$f^{\mathrm{T}} = \frac{3}{2}\left(\frac{\mathrm{d}^2V}{\mathrm{d}r^2}\right)_0 \cos^2\Theta \tag{4}$$

where Θ is the angle between the I—I bond between the layers and the basal plane. Raman spectra under pressure provide information about the variation of the force constant with pressure. Combining the Raman data and X-ray analysis under pressure, the dependence of f^{T} on the I—I distance has been determined. Fitting of the calculated $f^{\mathrm{T}} - r$ relation to the experimental data, using B, C and ρ as adjustable parameters, provides the best fit parameters, $C_{\mathrm{I-I}} = 0.7 \times 10^{-57}$ erg cm^6, B $= 3.1 \times 10^{-3}$ erg and $\rho = 0.32$ Å. Substituting the value of $C_{\mathrm{I-I}}$ into Eq. (2), one gets $\alpha_{\mathrm{I}} = 4.7 \times 10^{-24}$ cm^3. This value is in fair agreement with the polarizability of iodine obtained from infrared reflection spectrum ($\alpha = 5.6 \times 10^{-24}$ cm^3). This agreement led to the conclusion that van der Waals interaction mainly contributes to the interlayer interaction in CdI_2.

A similar analysis has been made for SnS_2, which is isomorphic to CdI_2. However, the polarizability of sulphur obtained from the pressure Raman measurement $\alpha = 12.0 \times 10^{-24}$ cm^3 is much larger than the value obtained from other measurement $\alpha = 3.8 \times 10^{-24}$ cm^3. This result suggests that for SnS_2 covalent or ionic bondings also contribute to the interlayer interaction.

(iii) The Dispersion of Acoustic Phonons in Layered Crystals

The restoring force for the accoustic phonons propagating along the direction perpendicular to the layer arises from the interlayer forces. Hence, the analysis of the dispersion curves of the accoustic phonons is desirable for a better understanding of the nature of the interlayer forces.

A direct way of obtaining phonon dispersion curves is neutron scattering. Usually, the Raman scattering gives only the phonon frequencies at Γ point (q = 0). However, phonon dispersion can be estimated from Raman measurements of the polytypes: Layered crystals which have more than one layer in the unit cell, i. e., long period polytypes, show rigid layer modes in the

Raman scattering. Since the rigid layer modes correspond to the acoustic phonon modes at certain positions in the Brillouin zone of the basic polytype (single-layer polytype), the phonon dispersion curves of the basic polytype can be inferred from the measured frequencies of the rigid layer modes in polytypes. Recently, the rigid layer modes of various polytypes of CdI_2 have been observed by Nakashima *et al.* and dispersion curves of transverse modes have been derived.[5] Figure 1 shows the dispersion curves of TA and TO phonons propagating along the c-direction in 2H—CdI_2.

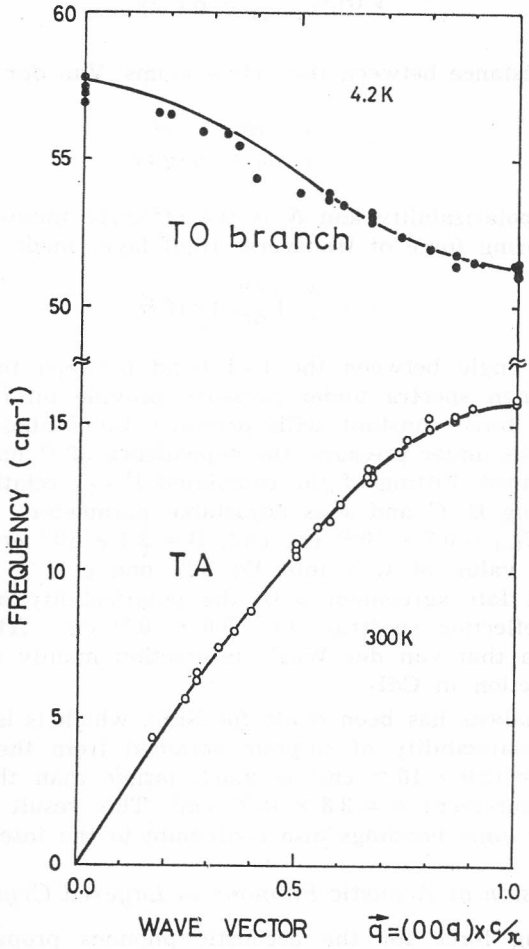

Figure 1. Dispersion curves of transverse acoustic and optic phonons in the [0, 0, ζ] direction of 2H—CdI_2, which are estimated from the frequencies of the rigid layer modes in various polytypes.[5] Solid lines are calculated from the linear chain model using force constant values taken in the text.

The dispersion relation of the accoustic branch is approximated by

$$\omega^2 = \frac{M}{2}\,[f_1\,(1 - \cos qc) + f_2\,(1 - \cos 2qc)] \tag{5}$$

where M is the mass of the unit layer and f_1 and f_2 are the force constants between the nearest and second nearest neighbour layers, respectively. Fitting Eq. (5) to the experimental values by adjusting f_1 and f_2 provides the best fit values, $f_1 = 1.35 \times 10^3$ dyn/cm and $f_2 = -60$ dyn/cm. A number of folded TA modes have been observed by Raman scattering in CdI_2[5], PbI_2[26], SnS_2[27], GaSe[28] and so on. The data are in good agreement with the dispersion relation obtained from the neutron scattering measurement. Interlayer forces f_1 and f_2 are obtained from fitting Eq. (5) to the experimental dispersion relation for GaS, GaSe, CdI_2, SnS_2, TiS_2, NbS_2 and MoS_2. The ratio of f_2 to f_1 for the transverse acoustic mode is less than 6% for these crystals.[1] This result indicates that the interlayer forces are predominantly short range ones and the contribution from long range force is small. If we assume, for simplicity, that the restoring force for the acoustic modes is the nearest neighbour layer force, the interlayer force is evaluated from the frequencies of the observed rigid layer modes. Table I lists the restoring forces of the transverse modes thus determined for some groups of layered crystals. It is to be noted that if the crystal structures are the same and the anions contributing to the interlayer forces belong to the same group in the periodic table, the interlayer forces are the same.

Layered crystals whose unit cell contains only one layer do not show rigid layer modes in Raman spectra. In this case, the strength of the interlayer forces can be derived from Brillouin measurement. The interlayer forces

TABLE I

Interlayer Forces for Shear Type Vibration Which are Determined From the Frequencies of the Rigid Layer Modes

materials	restoring forces (10^3 dyn/cm)
CdI_2 and $CdCl_2$ type metal halides	1.0—1.4
MX_2 type metal dichalcogenides (M = Sn, Ti, W, Nb, Ta, Mo)	2.0—3.3
GaS, GaSe, InSe	1.4—1.9
Graphite, BN	0.6—1.0
red HgI_2	~ 2.0
As_2S_3, As_2Se_3	1.8—4.0

obtained from the Brillouin measurement for layered crystals with multi--layers per unit cell (CdI_2, PbI_2 and GaSe) were in fair agreement with those obtained from the measurement of the rigid layer modes.[29] The force derived from recent ultrasonic measurements for GaS[30] also rendered agreement with that obtained from the rigid-layer-mode measurements.

(iv) Structure Identification

So far, the structures of polytypes of layered crystals have been determined mainly by X-ray diffraction analysis. Recently, it has been proved that the Raman intensity analysis is also useful for identifying the polytype structure.[5] Long period polytypes show a number of rigid layer modes,

whose relative intensity depends strongly on the stacking of layers. This means that the stacking sequences can be determined from the Raman intensity of the folded modes.

Raman scattering intensity of phonon modes is proportional to the square of Raman polarizability tensors $\partial\alpha/\partial Q$:

$$W = A \frac{n(\omega_\lambda) + 1}{\omega_\lambda} \left[e_i \cdot \frac{\partial \alpha}{\partial Q_\lambda} \cdot e_s \right]^2 \tag{6}$$

where $n(\omega_\lambda) + 1$ is the thermal population factor, e_i and e_s are the polarization vectors of incident and scattered light, respectively. $\partial\alpha/\partial Q$ is related to the atomic displacement vectors:[31]

$$\frac{\partial \alpha_{\varrho\sigma}}{\partial Q_\lambda} = \alpha'_{\varrho\sigma}(\lambda) = \sum_n \left\{ \frac{\partial [\alpha_n]_{\varrho\sigma}}{\partial x_i} \Delta \overset{\lambda}{u}_{ix} + \frac{\partial [\alpha_n]_{\varrho\sigma}}{\partial y_i} \Delta \overset{\lambda}{u}_{iy} + \frac{\partial [\alpha_n]_{\varrho\sigma}}{\partial z_i} \Delta \overset{\lambda}{u}_{iz} \right\} \tag{7}$$

where $\partial [\alpha_n]_{\varrho\sigma}/\partial x_i$ is the Raman tensor of n-th bond for the displacement along the x direction of the i-th atom related to the n-th bond. $\Delta u_n = u_i - u_p$ is the relative displacement of two end atoms of the n-th bond, which is obtained by solving the equation of motion.

For the rigid layer mode of CdI_2, the whole atoms within a layer move as rigid body. Accordingly, only the relative displacement between iodine atoms in the adjacent layers contributes to its Raman polarizability. On the other hand, for TO mode the relative displacement between iodine and Cd atoms within a layer contributes to the Raman polarizability.

The I—I bonds contributing to the bond Raman polarizability tensor of the folded TA modes are classified into two groups. (One group is A—B, B—C and C—A bonds and the other A—C, B—A and C—B bonds where A, B and C are the positions of iodine atoms.) Components α'_{xx}, α'_{yy} and α'_{xy} of the bond Raman polarizability tensor are the same in magnitude and opposite in sign for the two groups. Hence Eq. (7) is reduced to a simple form

$$\alpha'_{\varrho\sigma}(\lambda) = \frac{C}{m} \sum_s \pm \Delta u_s(\lambda), \qquad \varrho, \sigma = x, y \tag{8}$$

where m is the number of layers in a unit cell, and $u_s(\lambda)$ is the relative displacement of the s- and (s + 1)-th atoms for the λ-th mode. Eq. (8) shows that to the first order approximation the relative Raman intensity of the folded TA modes is independent of the values of the bond Raman polarizability. Atomic displacements are calculated from a lattice dynamical model. We have calculated the Raman intensity profiles of the folded TA modes and also TO modes using a linear chain model. Figure 2 shows a comparison of the calculated intensities and observed spectra for 12H, 16H and 22H polytypes. As seen in the figure, the calculated intensities agree quantitatively with the observed intensity profiles. This result indicates that analysis of the Raman intensity of the folded modes can be used to determine the structure of the polytypes of CdI_2. The Raman scattering analysis of the polytype structures has been extended to polytypes of other materials.

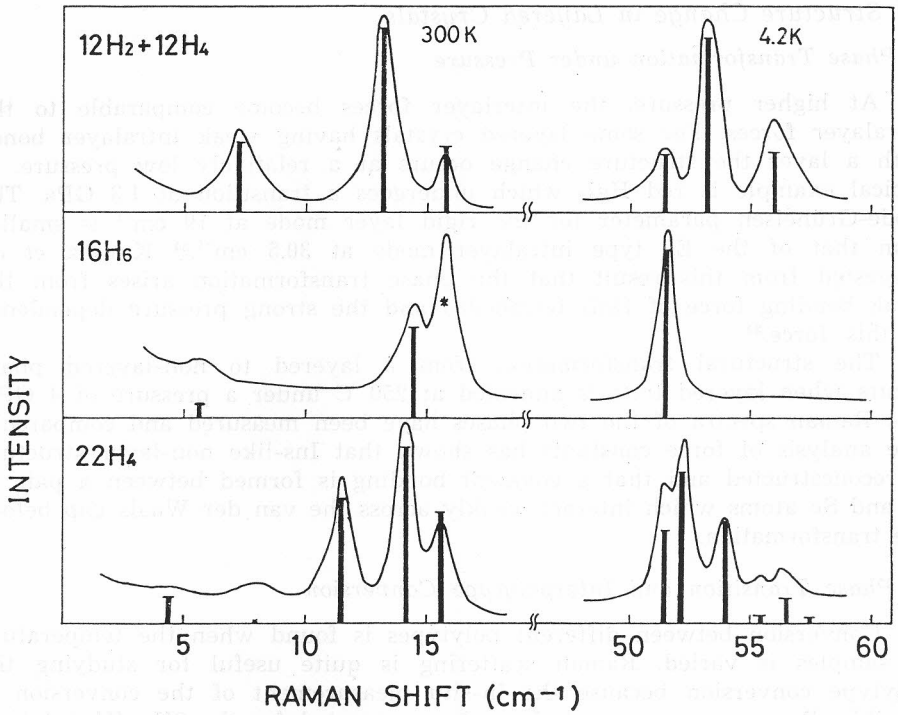

Figure 2. The calculated and observed Raman intensities of the folded modes are compared for polytypes ($12H_2 + 12H_4$), $16H_6$ and $22H_4$.[5] The height of the vertical bars represents the calculated intensity. The band with asterisk (*) is due to the mixture of 4H.

It has been often found that some Raman active modes are too weak to be observed. They are called missing modes. The study of the Raman intensity for layer crystals has shown that Raman polarizability of some modes becomes zero due to cancellation of bond Raman polarizabilities in a unit cell, even if these modes are group-theoretically allowed.[32] These modes may correspond to the missing modes.

A layer of GaSe is built from stacking of Se-Ga-Ga-Se atomic planes. The ε-GaSe crystal shows four strong Raman bands except for TO-LO splitting and the rigid layer modes. For these strong modes the atomic movement accompanies a variation in the Ga-Ga bond length, whereas the intensities of the modes which are related to the Ga-Se band are weak. This fact suggests that the Ga-Ga bond greatly contributes to the Raman polarizability and the electronic charge is concentrated in between the two Ga planes within a layer.[32] Recent studies on electron distribution in GaSe have demonstrated that the electronic charge distribution has a character of Ga_2 diatomic molecule and is concentrated between two Ga planes.[33] Analysis of the relative Raman intensities would provide information about the bonding nature of layered crystals.

(v) Structure Change in Layered Crystals

a) Phase Transformation under Pressure

At higher pressure, the interlayer forces become comparable to the intralayer forces. For some layered crystals having weak intralayer bonds with a layer the structure change occurs at a relatively low pressure. A typical example is red HgI_2 which undergoes a transition at 1.3 GPa. The mode-Grüneisen parameter for the rigid layer mode at 19 cm^{-1} is smaller than that of the Eg type intralayer mode at 30.5 cm^{-1}.[34] Kuroda *et al.* suggested from this result that the phase transformation arises from the weak bending force of HgI_4 tetrahedra and the strong pressure dependence of this force.[34]

The structural transformation from a layered to non-layered phase occurs when layered InSe is annealed at 250 °C under a pressure of 4 GPa. The Raman spectra of the two phases have been measured and compared.[35] The analysis of force constants has shown that Ins-like non-layer structure is reconcstructed and that a covalent bonding is formed between a pair of In and Se atoms which interact weakly across the van der Waals gap before the transformation.

b) Phase Transition and Interpolytype Conversion

Conversion between different polytypes is found when the temperature of samples is varied. Raman scattering is quite useful for studying the polytype conversion because the in-situ measurement of the conversion is possible. Raman measurements have been reported for the 2H—4H polytype conversion in PbI_2 on heating[36] and 2H—3R conversion in NbS_2 on cooling.[37]

A number of transition metal dichalcogenides undergo CDW phase transition. It reflects the low dimensional structure of a Fermi surface. Raman scattering measurements have been made to elucidate the mechanism of the CDW phase transition.[38] Anomalous temperature variation of Raman frequencies has been found at around the temperature of the transition between different phases (normal, commensurate and incommensurate phases).

A strong two-phonon band has been observed in 2H-polytype Group Va transition metal dichalcogenides which show the CDW phase transition (2H-$NbSe_2$, -$TaSe_2$ and -TaS_2).[38] This band arises from Kohn anomaly modes at $-2k_f$ and $2k_f$. Maldague and Tsang[39] and Klein[40] have shown that its strong intensity is related to the singular behaviour of susceptibility which causes the softening of the Kohn anomaly mode. From the analysis of the second order Raman spectra the temperature dependence of electronic susceptibility was obtained for 2H-$TaSe_2$[38], 2H-$NbSe_2$[38] and 4Hb-$TaSe_2$.[41]

c) Layered Crystals Having Stacking Disorder

Raman scattering and X-ray diffraction have been studied on CdI_2 crystals with stacking disorder. For disordered CdI_2 the structures of individual layers are the same and only the stacking of the layers is disordered. Hence, disordered CdI_2 can be regarded as an extreme case of very large period polytypes, in which the unit cell is infinite in size and its Brillouin zone becomes just the point $q = 0$. Under this simple assumption, the inten-

sity profiles of the Raman and X-ray scatterings are calculated using various models of disordered CdI_2. The two profiles are well explained by the same model structure.[42] This result suggests that the structure of disordered layered crystals can be understood in more detail by the combination of Raman scattering and X-ray diffraction analyses.

Raman spectral profiles are also calculated for 4H hase disordered polytypes which contain only one kind of fault. The calculated folded TA mode, which appears at 15.8 cm^{-1} for the pure 4H polytype, shifts to low frequency side, broadens and shows an asymmetric band shape as the number of faults increases.[42] This result is consistent with the observed spectra of disordered CdI_2.

IV. INTERCALATION COMPOUNDS

Some layer compounds can be intercalated with various ions or molecules between their layers (van der Waals gap). The intercalation reaction is expected as a new synthetic method for obtaining materials with desired physical properties by an apropriate choice of guest and host materials. Raman scattering is used to study the change of the host and guest induced by the intercalation reaction from the vibrational point of view. Here, we take up the intercalation compounds of graphite, transition metal dichalcogenides (MX_2) and metal phosphorus trisulfides (MPS_3).

(i) Graphite Intercalation Compound (GIC)

The phonon dispersion curves of graphite have been recently determined by Raman, infrared and neutron studies. The interlayer forces are weaker than the intralayer forces by two or three orders of magnitude. The GIC shows a staging phenomenon; guest ions or molecules are intercalated every n graphite layers (stage n), where n depends on the reaction condition. The intralayer E_{2g} mode is sensitive to the staging.[43] When the staging number n is larger than 3, the E_{2g} mode splits into doublets, e. g. E_{2g}^0 and $\hat{E}_{2g}$. The frequencies of these modes are a linear function of the inverse staging number n^{-1}. The frequency of the $\hat{E}_{2g}$ mode shifts upwards (downwards) with n^{-1} if the intercalant is an accepter (donor). In the case of $n \geq 3$, there are two types of graphite layers in GIC; the »graphite bounding layers« adjacent to the intercalant and the »graphite interior layers« which have only graphite nearest neighbouring layers. The $\hat{E}_{2g}$ and E_{2g}^0 modes are assigned to the intralayer vibrations of the bounding and interior graphite layers, respectively.

Using the staging dependence of the E_{2g}-mode frequency, Nishitani *et al.*[44] studied the dependence of the Raman spectra on the sample position and time during the intercalation reaction of H_2SO_4 in situ. They observed narrow stage boundaries and their movement into the internal region of the graphite crystals as the time passes. McNeil et al.[45] also observed the stage boundaries in $SbCl_5$-, Br_2- and $FeCl_3$—GIC by Raman microprobe. They recorded depletion of the intercalant within 10 μm from the sample edge

for $SbCl_5$-GIC, which is explained in terms of the thermal contraction of the intercalant after the intercalation reaction is completed.

(ii) Intercalation Compounds of Transition Metal Dichalcogenides

A large number of molecules and ions are intercalated into transition metal dichalcogenides (MX_2). As a driving force for the intercalation reaction, a charge transfer (CT) from guests to hosts has been proposed. If CT occurs, the Fermi surface changes and the CDW is either stabilized or suppressed. 1T-TaS_2 undergoes the CDW phase transition from the $\sqrt{13}\,a \times \sqrt{13}\,a \times 13\,c$ commensurate phase to the nearly commensurate phase at about 200 K, where a and c represent lattice constants in the normal phase. Figure 3 shows the Raman spectra of 1T-TaS_2 and TaS_2 intercalated with ethylenediamine (EDA) at ~ 100 K and room temperature.[3] The spectrum of 1T-TaS_2 changes drastically by phase transition; the complicated structure associated with superstructure in the commensurate phase disappears and the spectrum becomes broad in the nearly commensurate phase. Reversely, the complicated

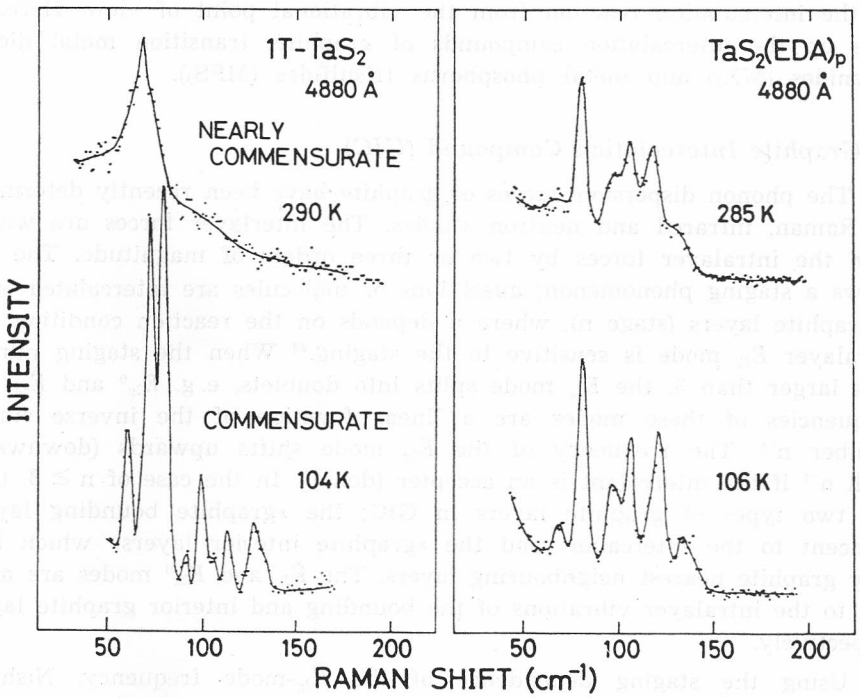

Figure 3. Raman spectra of pure and EDA intercalated 1T—TaS_2 measured at RT and ~ 100 K.[3]

structure observed at ~ 100 K still remains at room temperature for TaS_2 $(EDA)_p$ ($p \approx 1/4$). This indicates that the commensurate CDW is stabilized by intercalation.

Raman spectra of 2H-TaS_2 and 1T-TiS_2 intercalated with Ag,[46-48] and 2H-$NbSe_2$ intercalated with Fe[49] were measured and new bands were found to appear in the low frequency region. If the concentration of intercalated atoms is 1/4 or 1/3 per one MX_2, metal atoms intercalated periodically in the plane induce superstructure in the host lattice. The new bands were interpreted in terms of the zone-folding of the phonon branches within the basal plane.

Folded modes have not been observed so far for 2H-MX_2 intercalated with organic molecules even when the intercalated molecules form superlattices commensurate with the host lattice. This fact indicates that the interaction between the MX_2 layer and organic molecules is weak compared with that between the MX_2 layer and intercalated metal ions. However, a considerable upshift of the E_g mode was observed for most of the 2H-MX_2-organic molecule systems.[1] This shift is thought to be caused by the CT.

(iii) Metal Phosphorus Trisulfide (MPS_3)

Metal phosphorus trisulfides crystallize in layered structures quite similar to those of MX_2. Each layer can be regarded as being composed of $P_2S_6^{4-}$ units and metal ions. Some of MPS_3 are transparent in the visible light region and suitable for Raman scattering studies.

Recently, pyridine was found to be intercalated in $MnPS_3$.[4] The intercalation is completely reversible in contrast to other MPS_3-intercalant systems, in which metal vacancies are formed in the host layers by the intercalation (substitution-intercalation reaction). The Raman spectrum of $MnPS_3$ consists of the internal vibration of the $P_2S_6^{4-}$ molecules, and the rotation and translation of $P_2S_6^{4-}$ and Mn^{2+}. The spectral feature corresponding to the internal vibrations of $P_2S_6^{4-}$ is retained after the intercalation of pyridine, whereas the vibrational structure corresponding to the external modes of $MnPS_3(pyridine)_{4/3}$ is considerably different from those of $MnPS_3$. This indicates that the relatively weak bonds between the Mn and S atoms are affected by the intercalation.

In the MPS_3-organic molecule systems, the internal vibrations of the guest molecules are usually observed in the Raman spectra.[50-53] The $MnPS_3$--pyridine system is of particular interest since the spectra of pyridine have been investigated in various circumstances so far and then one can obtain information on the state of intercalated pyridine by comparing the internal vibration of pyridine with that of pyridine in various states. Figure 4 shows the spectra of $MnPS_3(pyridine)_{4/3}$, liquid pyridine and aqueous solution of pyridine in the ring stretching vibration region.[4] It is well known that the ring stretching vibrations of liquid pyridine at 992 (ν_1) and 1032 (ν_6) cm^{-1} shift upwards when it is chemisorbed on silver surfaces (adsorbed by the chemical bonds), hydrogen-bonded or coordinated to metal ions, whereas the frequencies of these modes in physisorbed pyridine are essentially the same as those of liquid pyridine. The splitting of the ν_1 and ν_6 modes for

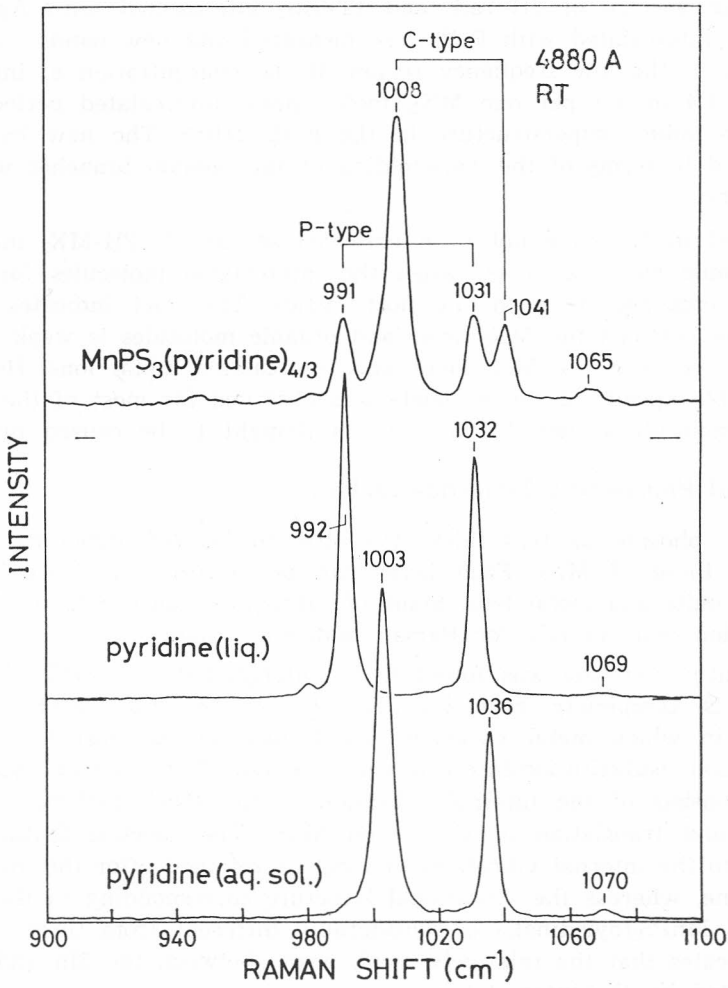

Figure 4. Raman spectrum of $MnPS_3(pyridine)_{4/3}$ in the ring stretching vibration region of pyridine.[4] Raman spectra of liquid pyridine and aqueous solution of pyridine are also shown for comparison. Bands denoted by P and C correspond to the modes of physisorbed and chemisorbed pyridine, respectively.

$MnPS_3(pyridine)_{4/3}$ is caused by the existence of two types of pyridine between the layers; one corresponding to the chemisorption and the other the pysisorption.

REFERENCES

1. S. Nakashima, M. Hangyo, and A. Mitsuishi, *Vibrational Spectroscopy of Layered Materials*, in: J. R. Durig (Ed.), *Vibrational Spectra and Structure*, A Series of Advances Vol. 14, Amsterdam, Elsevier, 1985. pp. 305—431.
2. T. J. Wieting and J. L. Verble, *Infrared and Raman Investigations of Long-Wavelength Phonons*, in: T. J. Wieting and M. Schlüter, (Ed.), *Physics and Chemistry of Materials with Layered Structures*, Vol. 3, Dordrecht, Reidel, 1979, pp. 321—407.

3. M. Hangyo, S. Nakashima, and A. Mitsuishi, *Ferroelectrics* **52** (1983) 151.
4. M. Hangyo, S. Nakashima, A. Mitsuishi, K. Kurosawa, and S. Saito, *Solid State Commun.* **65** (1988) 419.
5. S. Nakashima, H. Katahama, Y. Nakakura, A. Mitsuishi, and B. Pałosz, *Phys. Rev. B* **31** (1985) 6531.
6. H. Kuzmany, *Phys. Stat. Sol. (b)* **97** (1980) 521.
7. I. Harada, Y. Furukawa, M. Tasumi, H. Shirakawa, and S. Ikeda, *J. Chem. Phys.* **73** (1980) 4746.
8. E. Mulazzi, G. P. Brivio, E. Faulques, and S. Lefrant, *Solid State Commun.* **46** (1983) 851.
9. G. P. Brivio and E. Mulazzi, *Phys. Rev. B* **30** (1984) 876.
10. D. N. Batchelder, R. J. Kennedy, D. Bloor, and R. J. Young, *J. Polym. Sci. Polym. Sci. Ed.* **19** (1981) 677.
11. M. L. Shand, R. R. Chance, M. LePostollec, and M. Schott, *Phys. Rev. B* **25** (1982) 4431.
12. T. J. Wieting, A. Grisel, and F. Lévy, *Physica* **B105** (1981) 366.
13. S. P. Gwet, Y. Mathey, and C. Sourisseau, *Phys. Stat. Sol. (b)* **123** (1984) 503.
14. H. J. Stolz, A. Otto, and L. Pintschovius, *On the Interaction between Chains in $(SN)_x$*, in: M. Balkanski, R. C. C. Leite, and S. P. S. Porto (Ed.), *Proc. 3rd Int. Conf. on Light Scattering in Solids,* Paris, Flammarion, 1976, pp. 737—741.
15. J. C. Tsang, C. Herman, and M. W. Shafer, *Phys. Rev. Lett.* **40** (1978) 1528.
16. S. Sugai, *Phys. Rev.* **B29** (1984) 953.
17. T. Sekine, T. Seino, M. Izumi, and E. Matsuura, *Solid State Commun.* **53** (1985) 767.
18. I. Ohana, D. Schmeltzer, D. Shaltiel, Y. Yacoby, and A. Mustachi, *Solid State Commun.* **54** (1985) 747.
19. A. Zwick, M. A. Renucci, P. Gressier, and A. Meerschaut, *Solid State Commun.* **56** (1985) 947.
20. S. Sugai, M. Sato, and S. Kurihara, *Phys. Rev. B* **32** (1985) 6809.
21. E. F. Steigmeier, R. Loudon, G. Harbeke, H. Auderset, and G. Scheiber, *Solid State Commun.* **17** (1975) 1447.
22. G. Travaglini, I. Mörke, and P. Wachter, *Solid State Commun.* **45** (1983) 289
23. S. Kurihara, *J. Phys. Soc. Jpn.* **48** (1980) 1821.
24. R. Zallen, *Phys. Rev. B* **9** (1974) 4485.
25. H. Katahama, S. Nakashima, A. Mitsuishi, M. Ishigame, and H. Arashi, *J. Phys. Chem. Solids* **44** (1983) 1081.
26. W. M. Sears, M. L. Klein, and J. A. Morrison, *Phys. Rev. B* **19** (1979) 2305.
27. A. J. Smith, P. E. Meek, and W. Y. Liang, *J. Phys. C* **10** (1977) 1321.
28. A. Polian, K. Kunc, and A. Kuhn, *Solid State Commun.* **19** (1976) 1079.
29. S. Nakashima, H. Katahama, M. Daimon, and A. Mitsuishi, *Solid State Commun.* **31** (1979) 913.
30. M. Gatulle, M. Fisher, and A. Chevy, *Phys. Stat. Sol. (b)* **119** (1983) 327.
31. S. Nakashima, H. Katahama, Y. Nakakura, and A. Mitsuishi, *Phys. Rev. B* **33** (1986) 5721.
32. S. Nakashima and M. Balkanski, *Phys. Rev. B* **34** (1986) 5801.
33. See C. Y. Fong and M. Schlüter, *Electronic Structure of Some Layer Compounds,* in: T. J. Wieting and M. Schlüter (Ed.), *Physics and Chemistry of Materials with Layer Structures,* Dordrecht, Reidel, 1979, pp. 145—318.
34. N. Kuroda, T. Iwabuchi, and Y. Nishina, *J. Phys. Soc. Jpn.* **52** (1983) 2419.
35. N. Kuroda, Y. Nishina, H. Iwasaki, and Y. Watanabe, *Solid State Commun.* **38** (1981) 139.
36. R. Zallen and M. L. Slade, *Solid State Commun.* **17** (1975) 1561.
37. W. G. McMullan and J. C. Irwin, *Phys. Stat. Sol. (b)* **129** (1985) 465.

38. See a review paper, S. Sugai, *Phys. Stat. Sol. (b)* **129** (1985) 13.
39. P. F. Maldague and J. C. Tsang, *Effect of Incipient Charge Density Waves on Second-Order Raman Spectroscopy*, in: M. Balkanski (Ed.), *Proc. 4th Int. Conf. on Lattice Dynamics*, Paris, Flammarion, 1978, pp. 602—605.
40. M. V. Klein, *Phys. Rev. B* **24** (1981) 4208.
41. T. Nakashizu, T. Sekine, K. Uchinokura, and E. Matsuura, *J. Phys. Soc. Jpn.* **55** (1986) 672.
42. S. Nakashima, Y. Nakakura, and B. Pałosz, to be published.
43. M. S. Dresselhaus and G. Dresselhaus, *Light Scattering in Graphite Intercalation Compounds*, in: M. Cardona and G. Guntherrodt (Ed.), *Light Scattering in Solids III, Topics in Applied Physics* Vol. **51**, Berlin, Springer-Verlag, 1982, pp. 3—57.
44. R. Nishitani, Y. Sasaki, and Y. Nishina, *J. Phys. Soc. Jpn.* **56** (1987) 1051.
45. L. E. McNeil, J. Steinbeck, L. Salamanca-Riba, and G. Dresselhaus, *Phys. Rev. B* **31** (1985) 2451.
46. W. G. McMullan and J. C. Irwin, *Canad. J. Phys.* **62** (1984) 789.
47. W. K. Unger, J. M. Reyes, A. E. Curzon, J. C. Irwin, and R. F. Frint, *Solid State Commun.* **28** (1978) 109.
48. R. Leonelli, M. Plischke, and J. C. Irwin, *Phys. Rev. Lett.* **45** (1980) 1291.
49. C. M. Pereira and W. Y. Liang, *J. Phys. C* **18** (1985) 6075.
50. Y. Mathey, R. Clement, C. Sourisseau, and G. Lucazeau, *Inorg. Chem.* **19** (1980) 2773.
51. C. Sourisseau, J. P. Forgerit, and Y. Mathey, *J. Phys. Chem. Solids* **44** (1983) 119.
52. O. Poizat and C. Sourisseau, *J. Phys. Chem.* **88** (1984) 3007.
53. O. Poizat, C. Sourisseau, and Y. Mathey, *J. .Chem. Soc., Faraday Trans. I* **80** (1984) 3257.

SAŽETAK

Karakterizacija niskodimenzijskih materijala Ramanovom spektroskopijom

S. Nakashima i M. Hangyo

Ovaj članak daje pregled najnovijeg napretka studija Ramanova raspršenja na jedno- i dvodimenzijskim materijalima. Opisana su vibracijska svojstva niskodimenzijskih kristala i sažeto prikazane različite metode karakterizacije ovakvih kristala. Prikazani su najnoviji eksperimentalni rezultati na polimernim kristalima, anorganskim lančastim kristalima, slojevitim kristalima i kristalima s uklopljenim slojevima.